Chinese Chemical Letters 33 (2022) 4664–4668

Contents lists available at ScienceDirect

Chinese Chemical Letters

journal homepage: www.elsevier.com/locate/cclet

Construction of one Ru_2W_{12}-cluster and six lacunary Keggin tungstoarsenate leading to the larger Ru-containing polyoxometalate photocatalyst

Huafeng Li, Mengnan Yang, Zelong Yuan, Yahao Sun, Pengtao Ma, Jingyang Niu*, Jingping Wang*

Henan Key Laboratory of Polyoxometalate Chemistry, College of Chemistry and Chemical Engineering, Henan University, Kaifeng 475004, China

ARTICLE INFO

Article history:
Received 30 November 2021
Revised 23 December 2021
Accepted 28 December 2021
Available online 4 January 2022

Keywords:
Ru-containing polyoxometalate
Photocatalyst
Oxidation
Azoxy compounds
Durability

ABSTRACT

Construction of two Ru^{III} cations and six lacunary Keggin fragments resulted in a novel Ru_2W_{12}-cluster $\{(RuO_6)_2(WO_3)_{12}(H_2O)_{12}\}$ bridged polyoxometalate, $NaH_{11}[(RuO_6)(AsW_9O_{33})_3\{(W_6O_3)(H_2O)_6\}]_2$ $53H_2O$ (NaH_{11}·**1**·$53H_2O$), which represent the largest cluster in all the Ru-containing polyoxometalates. The most interesting characteristic is that the symmetry-related Ru_2W_{12}-cluster-based hexamers contain two windmill-shaped $[(RuO_6)(AsW_9O_{33})_3\{(W_6O_3)(H_2O)_6\}]$ trimers or the Ru_2W_{12} cluster was tightly wrapped by six segments of B-β-AsW_9O_{33}. The other remarkable feature is that there have one intriguing cubane structure: which is composed of the Ru(1, 2) and W(1, 28, 50, 51, 52, 53) atoms. The oxygenation reactions of anilines to azoxybenzenes was evaluated when NaH_{11}·**1**·$53H_2O$ served as effective catalyst by probing various reaction. The inherent redox property of oxygen-rich polyoxometalate surfaces and high photocatalytic activity of the Ru-containing metal cluster imbedded in NaH_{11}·**1**·$53H_2O$ provide sufficient driving force for the photocatalytic transformation from anilines to azoxybenzenes. The oxidation of anilines can be realized with higher selectivity to afford various azoxybenzene compounds. The durability test shows that Ru-doping catalyst displays excellent chemical stability during the photocatalytic process.

Large polyoxometalates (POMs) are of particular interest with fascinating structures combined with their rich electronic properties of oxygen-rich surfaces and manifold molecular characteristics have received much attention in catalysis, medicine, and material science [1–3]. A particularly interesting direction in this field is the introduction of transition metal (TM) centres form heterometallic 3d-4f clusters due to their unique properties arising from the interactions of 3d and 4f metal ions [4–6]. Currently, ruthenium as 3d metal is prominent among the elements with superior catalytic activity, with a broad substrates ranging from organic products to water [7]. Until now, a variety of TM cluster incorporated large POMs have been obtained and numerous large-cluster-shaped POMs are also now well-established such as $Cs_{20}[\{Nb_4O_6\}(Nb_3SiW_9O_{40})_4]$ [8], $Na_{22}Rb_6[\{Co_4(OH)_3PO_4\}_4(PW_9O_{34})_4]$ [9], $Na_{34}[\{Mn_{19}(OH)_{12}\}(SiW_{10}O_{37})_6]$ [10], $Na_{19}H_{26}[\{Ti(OH)_3\}_4Cl(P_2W_{15}Ti_3O_{62})_4]$ [11], $K_{12}Na_{16}[H_{56}Fe_{28}P_8W_{48}O_{248}]$ [12], $K_{12}Li_{13}[\{Cu_{20}Cl(OH)_{24}(H_2O)_{12}\}(P_8W_{48}O_{184})]$ [13], $K_{56}Li_{74}H_{14}[\{(P_2W_{14}Mn^{III}{}_4O_{60})(P_2W_{15}Mn^{III}{}_3O_{58})_2\}_4(P_8W_{48}O_{184})]$ [14], $(NH_4)_{20}[\{(Fe^{III}(H_2O))_{30}\}\{(W)W_5O_{21}(SO_4)\}_{12}(SO_4)_{13}(H_2O)_{34}]$ [15] and $[\{Ni^{II}{}_6(Tris)(en)_3(BTC)_{1.5}(PW_9O_{34})\}_8]$ [16]; however, isolable large Ru-containing complexes are rare, though the Ru-based POMs possess valuable photocatalytic performance [17,18]. Since the first mono-Ru-substituted POM $[(C_6H_{13})4N]_5[Ru(H_2O)SiW_{11}O_{39}]$ was made in 1989 [19], so far the largest structure of Ru-containing POMs is organic-inorganic hybrid $K_{16}Li_{11}[\{K(H_2O)\}_3\{Ru(p\text{-cymene})(H_2O)\}_4\{P_8W_{49}O_{186}(H_2O)_2\}]$ [20]. Thus, exploring giant Ru-containing POMs and investigating their superior catalytic properties still meet a severe challenge. To explore the optimal strategy for whether the large Ru-cluster can be tightly incorporated to specific POM frameworks form target compounds is very fascinating and challenging topic.

The above mentioned large-cluster-shaped POMs are generally obtained by reaction of TM with lacunary precursors elements under the conventional solutions conditions. However, the high-success hydrothermal synthesis strategy has been frequently used as the most promising method to make TM-containing POMs in the reaction systems of simple materials and trivalent Ru ions leading to a series of structural novel Ru-cluster bridged POMs [21]. The introduction of trivalence Ru ions with potential performance into this reaction system have greatly arouses our attention. In addi-

* Corresponding authors.
E-mail addresses: jyniu@henu.edu.cn (J. Niu), jpwang@henu.edu.cn (J. Wang).

https://doi.org/10.1016/j.cclet.2021.12.081
1001-8417/

tion, P and Si are frequently used as the central atoms in the many of the reported Ru-containing POMs, but only few As be seclected as the central atom. Considering all the above reasons, Na_2WO_4, $NaAsO_2$ and $RuCl_3$ were chosen as the starting material to make the desired Ru-containing POMs (Fig. S1 in Supporting information).

Fortunately, a novel Ru_2W_{12}-cluster bridged tungstoarsenate, $NaH_{11}[(RuO_6)(AsW_9O_{33})_3\{(W_6O_3)(H_2O)_6\}]_2$ $53H_2O$ (NaH_{11}·**1**·$53H_2O$), have been synthesized. NaH_{11}·**1**·$53H_2O$ have the large Ru_2W_{12} cluster and show the largest structure in all the Ru-containing POMs up to date, in which the Ru_2W_{12}-cluster was tightly trapped by six same units of B-β-AsW_9O_{33} (Figs. S2 and S3 in Supporting information). Most interestingly, the photocatalysis oxygenation coupling reaction of anilines be selected as model substrates due to the important application prospects in chemical industry [22,23]. Results indicate that NaH_{11}·**1**·$53H_2O$ is an effective photocatalyst for the preparation of azoxybenzenes from anilines with excellent yields and high selectivity. We infer the inherent redox property of oxygen-rich POMs surfaces and high photocatalytic activity of the Ru-containing metal cluster imbedded in NaH_{11}·**1**·$53H_2O$ provide a sufficient driving force for the photocatalytic transformation from anilines to azoxybenzenes, which can be verified by our experiments results and the fact that hardly target products are rapidly oxidized under light irradiation in the absence of photocatalysts.

Black block crystals of NaH_{11}·**1**·$53H_2O$ were prepared by the hydrothermal synthesis method of $NaWO_4{\cdot}2H_2O$, $NaAsO_2$ and $RuCl_3$ in water at 180 °C for 3 days (Fig. S1 in Supporting information). Though the $NaWO_4{\cdot}2H_2O$, $NaAsO_2$ and $RuCl_3$ were selected as the starting material, **1** is composed by six B-β-AsW_9O_{33} fragments (Fig. S2), suggesting that the polymerization reaction of W and As atoms to B-β-AsW_9O_{33} units should have taken place in the process of the reaction. As shown in Fig. 1a, **1** contains six B-β-AsW_9O_{33} fragments, two RuO_6 units, two $(W_6O_3)(H_2O)_6$ units. X-ray single-crystal structure analysis indicates that **1** owns a monoclinic Ru_2W_{12}-cluster hexamer $[(RuO_6)_2(AsW_9O_{33})_6\{(W_6O_3)_2(H_2O)_{12}\}]^{12-}$ (Figs. 1a-f and Table S1 in Supporting information), which consists of two symmetric **1a** trimers $[(RuO_6)(AsW_9O_{33})_3\{(W_6O_3)(H_2O)_6\}]^{6-}$ (Figs. 1c and f) *via* six μ_2-oxo bridges. Twelve coordination water molecules O(63, 65, 82, 103, 104, 123, 144, 185, 204, 208, 215, 217) (Fig. S3 in Supporting information) in **1** can further locked by bond valence sum (BVS) calculations (Table S3 in Supporting information) [24,25]. **1** displays two conspicuous features: the coresidency of six B-β-AsW_9O_{33} fragments (Figs. 1g-l), and the occurrence of an undiscovered hexagon-shaped Ru_2W_{12} cluster (Fig. S3a) that is incorporated to the framework of **1** and firmly stabilized by six trilacunary B-β-AsW_9O_{33} fragments. In the Ru_2W_{12} cluster, interestingly, eight octahedral distribution fashion of Ru(1,2) and W(1, 28, 50, 51, 52, 53) ions by corner-sharing form intriguing cubane structural Ru_2W_6 cluster $\{(RuO_6)_2(WO_3)_6(H_2O)_6\}$ (Figs. 1m and n), and another six W(4, 10, 27, 54, 55, 56) ions are absorbed on both sides of the cubane structure (Fig. S3). Another interesting feature of **1** is that the coexistence of six B-β-$AsW_{10}O_{37}$ units (Figs. 1g-l), and the occurrence of an undiscovered cubane-shaped Ru_2W_6 cluster that is incorporated to the framework of **1** and tightly wrapped by six lacunary B-β-$AsW_{10}O_{37}$ fragments. As to B-β-AsW_9O_{33} and B-β-$AsW_{10}O_{37}$, the latter is easy to aggregate by bridging oxygen formed $[(RuO_6)(AsW_{10}O_{34})_3(H_2O)_6]^{24-}$ trimers, which has been confirmed by the high-resolution electrospray ionization mass spectrometry (HR-ESI-MS), and two prominent peaks at m/z = 1627.34 and 2040.44 were assigned to the $[H_{19}(RuO_6)(AsW_{10}O_{34})_3(H_2O)_{18}(CH_3OH)_7]^{5-}$ (simulated 1627.35) and $[H_{20}(RuO_6)(AsW_{10}O_{34})_3(H_2O)_{30}(CH_3OH)\}]^{4-}$ (simulated 2040.42), clearly proves the stability of the trimers **1a** anions groups in methanol (Table S4 and Fig. S4 in Supporting information). The rational reason is that the B-β-$AsW_{10}O_{37}$ owns more exposed surface O atoms than the B-β-AsW_9O_{33} at vacant sites, which results in that the B-β-$AsW_{10}O_{37}$ as multidentate ligand can better enhance the stability of the products when they chelated to the *in situ* formed the larger Ru-containing cluster [21]. The B-β-$AsW_{10}O_{37}$ segment derived from the polymerization of lacunary Keggin unit B-β-AsW_9O_{33} by chelating a WO_6 group (Figs. 1g-l). Bond valence sum (BVS) calculations of **1** indicate that the oxidation states of the W, As, and Ru centers are +6, +3, and +3, respectively (Tables S3 in Supporting information), which were supported by the X-ray photoelectron spectra (Fig. 2a and Fig. S8 in Supporting information).

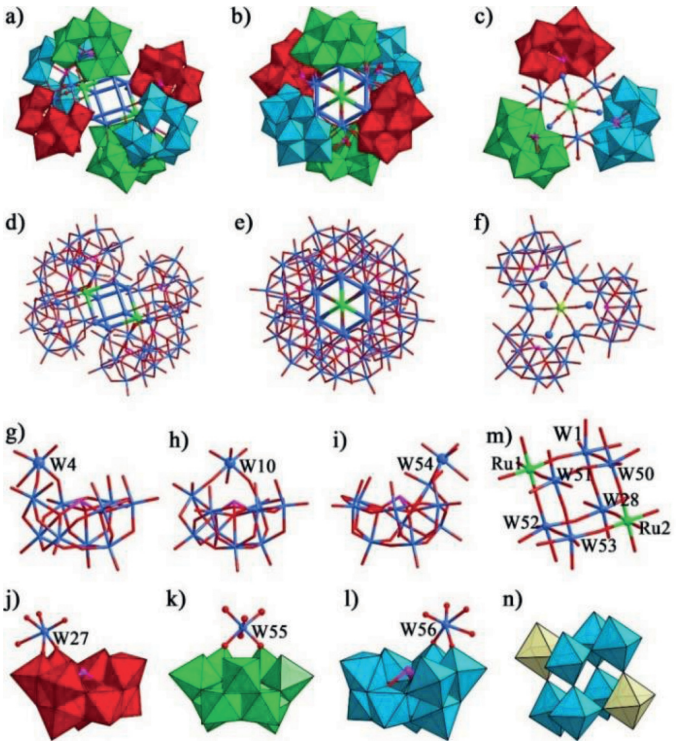

Fig. 1. Ball-and-stick and polyhedral representation of the structure: (a, b) **1** for different perspectives; (c) **1a**. Ball-and-stick representation of the structure: (d, e) **1** for different perspectives; (f) **1a**. Ball-and-stick representation of the structure: (g-i) Lacunary Keggin-type unit for **1a**. Ball-and-stick and polyhedral representation of the structure: (j-l) Lacunary Keggin-type unit for **1a**. (m) Ball-and-stick representation of Ru_2W_6 cluster. (n) Polyhedral representation of Ru_2W_6 cluster. Color codes: WO_6, red/bright green/sky blue octahedra; RuO_6, light yellow; W, light blue sphere; O, red sphere; Ru, bright green sphere; As, pink sphere.

The characteristic vibration patterns of the typical Keggin-type polyanions dominate the IR spectra of NaH_{11}·**1**·$53H_2O$ (Fig. S5 in Supporting information). Several strong characteristic bands were observed at 971, 906, 840 and 689 cm^{-1}, which can be attributed to the characteristic ν_{as}(As–O_a), ν_{as}(W–O_t), ν_{as}(W–O_b), and ν_{as}(W–O_c) [26,27]. Two strong absorption bands at about 3445 cm^{-1} and 1620 cm^{-1} are assigned to the stretching vibration of lattice water and OH group, respectively [28]. The experimental powder X-ray diffraction (PXRD) pattern of NaH_{11}·**1**·$53H_2O$ is in good agreement with the simulated patterns, suggesting the good phase purity of the sample (Fig. 2b) [29,30]. The UV/vis spectra of NaH_{11}·**1**·$53H_2O$ showed a characteristic absorption band around 480 nm (Fig. S6 in Supporting information), which is consistent with the presence of Ru causes the dominant oxygen-Ru responsive charge transfer [31]. The TG curves of NaH_{11}·**1**·$53H_2O$ indicate that the frameworks of NaH_{11}·**1**·$53H_2O$ can remain stable until 480 °C. (Fig. S7 in Supporting information) [32].

Table 1
Optimal reaction conditions.[a]

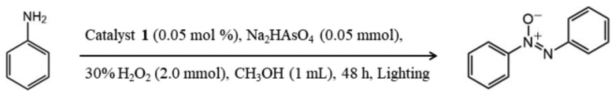

Entry	Catalyst	Yield (%) [b]
1	**1**	94.2
2	Na_2WO_4	66.0
3	$NaAsO_2$	16.8
4	$RuCl_3$	< 10
5	Blank	25.2
6	O_2 replacement H_2O_2	< 10
7	N_2 replacement H_2O_2	< 10
8	**1** (dark)	< 10

[a] NaH_{11}·**1**·53H_2O (0.05 mol%), substrate (1.0 mmol), methanol (1.0 mL), 30% H_2O_2 (2.0 mmol), Na_2HAsO_4 (0.05 mmol), 10 W white LED lamp, 48 h.
[b] GC yields for target product were based on naphthalene as internal standard.

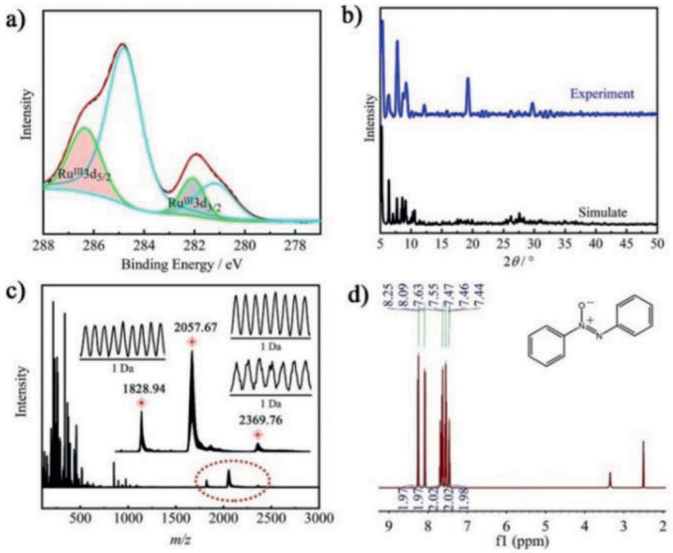

Fig. 2. (a) XPS spectra for Ru 3d of NaH_{11}·**1**·53H_2O. (b) PXRD pattern of NaH_{11}·**1**·53H_2O. (c) Negative ESI-MS spectrum of NaH_{11}·**1**·53H_2O in methanol. (d) ^{1}H NMR spectra for **2a** (500 MHz, DMSO).

Azoxybenzene compounds, as important chemical intermediate, have found tremendous applications in organic synthesis industry as organic dyes, photochemical switches, pharmaceuticals and food additives [33–35]. Aiming to prepare the valuable azoxybenzene derivatives, phenylamine was preferred as a model substrate to exploring ideal reaction conditions for the Ru-containing POM photocatalyzed oxidative coupling of aromatic amines in an environmentally greener processes. By employing 0.05 mol% of NaH_{11}·**1**·53H_2O in the presence of 2.0 mmol of H_2O_2 (30% in H_2O_2) in methanol for 48 h under 10 W LED exposure, we were surprised to found the formation of azoxybenzene as the target product with 80% yield (Table S6 in Supporting information). To produce more valuable target product with high selectivity, it is necessary to investigated various additives, such as Na_2CO_3, $NaHCO_3$, K_3PO_4, Na_2SO_4, Na_2SO_3, $Na_2S_2O_4$, $Na_2S_2O_8$, As_2O_3, $NaAsO_2$ and Na_2HAsO_4 (Table S6). Obviously, when 0.05 mmol of Na_2HAsO_4 was used, a significant amount of azoxybenzene (94.2% yield) was observed (Table 1, entry 1). This oxidative coupling reaction was accelerated slightly by increasing the molar weight of photocatalyst, then the ideal dosage could be locked in 0.05 mol% of NaH_{11}·**1**·53H_2O (Table S6). The photocatalyzed oxidative reaction worked in a variety of organic solvents (toluene, acetonitrile, dimethyl formamide, dichloromethane, methyl tert–butyl ether, ethanol, methanol), in which methanol giving the highest yield and selectivity (Table S7 in Supporting information). The HR-ESI-MS analyses were used to study catalyst stability, and three prominent peaks at m/z = 1828.94, 2057.67, and 2369.76 were assigned to the $[H_3(RuO_6)_2(AsW_9O_{33})_6\{(W_6O_3)_2(H_2O)_{12}\}]^{9-}$ (simulated 1828.92), $[H_4(RuO_6)_2(AsW_9O_{33})_6\{(W_6O_3)_2(H_2O)_{12}\}]^{8-}$ (simulated 2057.66) and $[H_5(RuO_6)_2(AsW_9O_{33})_6\{(W_6O_3)_2(H_2O)_{19}\}]^{7-}$ (simulated 2369.77), clearly proves the stability of the complete anions groups of NaH_{11}·**1**·53H_2O in methanol (Fig. 2c). Interestingly, performing the single catalyst, such as Na_2WO_4, As_2O_3 and $RuCl_3$, was also observe to promote the oxidative coupling reactions (Table 1, entries 2–4), however with pessimistic efficiency. No desired target product was detected in the absence of catalyst NaH_{11}·**1**·53H_2O under light irradiation (Table 1, entry 5). Besides, the photocatalytic coupling reaction was thoroughly lose efficacy when O_2 or N_2 were chosen as the replacement of H_2O_2, which indicates the hydrogen peroxide play a significant role in this reaction system (Table 1, entries 6 and 7). Furthermore, omitting the light from the reaction system led to a significant change in the reaction outcome (Table 1, entry 8). This result clearly confirmed that the transformation of phenylamine to azoxybenzene proceeded *via* a photocatalytic process. However, the photocatalytic activity was no considerable improvement in the transformation of the substrate as the temperature change from 30 °C to 50 °C (Fig. S9 in Supporting information). It further proved that the reaction was implemented by the light-driven rather than thermally driven. After comprehensive optimization with the relevant reaction parameters (Tables S6 and S7), we were delighted to found that 0.05 mol% NaH_{11}·**1**·53H_2O, with 0.05 mmol of Na_2HAsO_4 and 2.0 mmol of H_2O_2 as oxidant in 1 mL methanol under light irradiation was the ideal photocatalytic reaction condition (Table 1, entry 1).

With the best reaction conditions, the evaluation of general applicability was subsequently performed (Scheme 1). A variety of substituted anilines with both electron-withdrawing and electron-donating were fleetly transformed into the corresponding azoxybenzene in excellent isolated yields (Scheme 1, **3b**–**o**). Initially, the oxidation was performed with aniline leading to azoxybenzene with the highest isolated yield (Fig. 2d and Scheme 1, **2a**). However, anilines substituted with electron-donating groups (Me, Et, ^{i}Pr, *n*-Bu, C(Me)$_3$, OMe, OEt) led to lower yields of the isolated products (Scheme 1, **2b**–**2l**). Most impressively, various anilines substituted with electron-withdrawting (F, CF_3, Cl, Br) led to corresponding products **2m**–**2r** in high isolated yields. In summary, it showed that the electron-deficient group reduces the electron cloud density around the benzene ring and further accelerates the photocatalysis reaction process. Moreover, we also investigated the sensitivity of steric hindrance for the substituents position on the phenyl ring. Substituents at the *para* position products for electron-

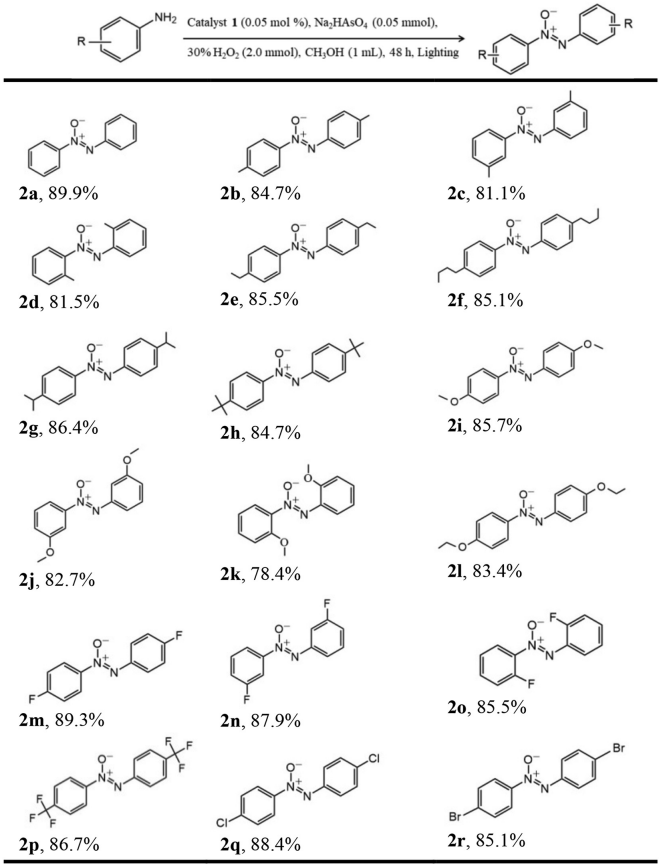

Scheme 1. Ru-catalysed oxidation reactions of anilines to azoxybenzenes. NaH_{11}·**1**·53H_2O (0.05 mol%), substrate (1.0 mmol), methanol (1.0 mL), 30% H_2O_2 (2.0 mmol), Na_2HAsO_4 (0.05 mmol), 10 W white LED lamp, 48 h. Isolated yields.

donating groups formed the relevant azoxy compounds in better yields than that of *ortho* and *meta* position products due to steric effects (Scheme 1, **2b**–**2d** and **2i**–**2k**). The same experimental results were obtained for the electron-withdrawting groups at different position products (Scheme 1, **2m**–**2o**). Most interestingly, a para-$C(Me)_3$ group as electron-donating substituent and a para-CF_3 group as electron-withdrawing substituent converted the target products with a good yields (Scheme 1, **2h** and **2p**).

Additionally, the scalability of the photocatalysis experiment was examined by oxidizing anilines on a ten-times scale, affording the desired azoxybenzene about 90% isolated yields, which further validated the good catalytic performance of NaH_{11}·**1**·53H_2O (Fig. 3a). The product of azoxybenzene is soluble in the reaction system, but can successfully be separated by extraction with normal hexane without interfering with the homogeneous catalyst. The reusability was tested by ten consecutive times for model substrate after the initial reaction (Fig. 3b). The experimental procedure was as follows: after the reaction, the solution was extracted to separate the product, the catalyst was remain in methanol phase, addition of 1 mmol anilines and 2.0 mmol 30% H_2O_2, restart directly for the next cycle. This extraction method shows that the soluble products also be effectively separated from the catalyst and to subsequently recycle the latter in the homogeneous reaction system. Simultaneously, the good time-resolved stability of polyanion **1** in methanol was proved for continuous usability (Fig. 3c).

In summary, we have demonstrated the capacity of largest Ru-containing POM catalyst NaH_{11}·**1**·53H_2O for the oxidation of anilines to achieve various azoxybenzene compounds. This protocol works with a wide range of substrates and tolerates a series of functional groups on the anilines. This work would enrich the POM

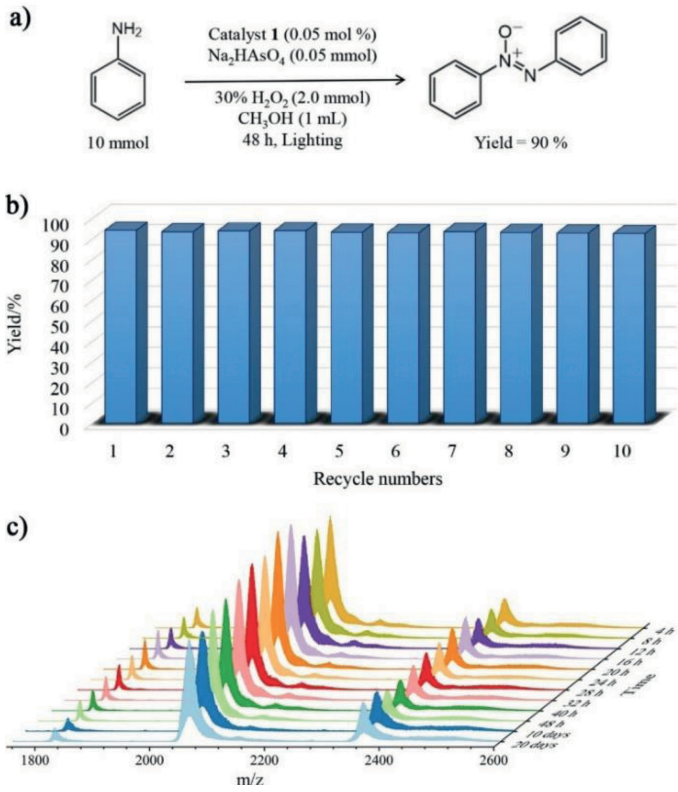

Fig. 3. (a) The large-scale experiment in presence of 0.05 mol% catalyst NaH_{11}·**1**·53H_2O. (b) Recycling experiments of NaH_{11}·**1**·53H_2O for the oxidation of anilines. (c) Time-resolved stability of the compound NaH_{11}·**1**·53H_2O in methanol.

family and provide an opportunity for the expansion of the potential applications of Ru-containing POM materials.

Declaration of competing interest

The authors declare that they have no known competing financial interests or personal relationships that could have appeared to influence the work reported in this paper.

Acknowledgment

This work was supported by the National Natural Science Foundation of China (Nos. 22171071, 22071044, 21771054, 21571050).

Supplementary materials

Supplementary material associated with this article can be found, in the online version, at doi:10.1016/j.cclet.2021.12.081.

References

[1] G.P. Yang, X.L. Zhang, Y.F. Liu, et al., Inorg. Chem. Front. 8 (2021) 4650–4656.
[2] S.T. Zheng, G.Y. Yang, Chem. Soc. Rev. 41 (2012) 7623–7646.
[3] G. Hu, W. Chang, S. An, B. Qi, Y.F. Song, Chin. Chem. Lett. (2021), doi:10.1016/j.cclet.2021.11.006.
[4] M.H. Du, X.Y. Zheng, X.J. Kong, L.S. Long, L.S. Zheng, Matter. 3 (2020) 1334–1349.
[5] V. Das, R. Kaushik, F. Hussain, Coord. Chem. Rev. 413 (2020) 213271.
[6] Y. Song, Y. Peng, S. Yao, et al., Chin. Chem. Lett. 33 (2022) 1047–1050.
[7] M. Pagliaro, S. Campestrini, R. Ciriminna, Chem. Soc. Rev. 34 (2005) 837–845.
[8] G.S. Kim, H. Zeng, D. VanDerveer, C.L. Hill, Angew. Chem. Int. Ed. 38 (1999) 3205–3207.
[9] M. Ibrahim, Y. Lan, B.S. Bassil, et al., Angew. Chem. Int. Ed. 50 (2011) 4708–4711.
[10] B.S. Bassil, M. Ibrahim, R. Al-Oweini, et al., Angew. Chem. Int. Ed. 50 (2011) 5961–5964.
[11] Y. Sakai, K. Yoza, C.N. Kato, K. Nomiya, Chem. Eur. J. 9 (2003) 4077–4083.

[12] B. Godin, Y.G. Chen, J. Vaissermann, et al., Angew. Chem. Int. Ed. 44 (2005) 3072–3075.
[13] S.S. Mal, U. Kortz, Angew. Chem. Int. Ed. 44 (2005) 3777–3780.
[14] X. Fang, P. Kögerler, Y. Furukawa, M. Speldrich, M. Luban, Angew. Chem. Int. Ed. 50 (2011) 5212–5216.
[15] A. Müller, E. Diemann, C. Kuhlmann, et al., Chem. Commun. (2001) 1928–1929.
[16] S.T. Zheng, J. Zhang, X.X. Li, W.H. Fang, G.Y. Yang, J. Am. Chem. Soc. 132 (2010) 15102–15103.
[17] H. Li, W. Chen, Y. Zhao, et al., Nanoscale 13 (2021) 8077–8086.
[18] Y. Liu, S.F. Zhao, S.X. Guo, et al., J. Am. Chem. Soc. 138 (2016) 2617–2628.
[19] R. Neumann, C. Abu-Gnim, J. Chem. Soc., Chem. Commun. (1989) 1324–1325.
[20] S.S. Mal, N.H. Nsouli, M.H. Dickman, U. Kortz, Dalton Trans. (2007) 2627–2630.
[21] L. Huang, S.S. Wang, J.W. Zhao, L. Cheng, G.Y. Yang, J. Am. Chem. Soc. 136 (2014) 7637–7642.
[22] G.S. Kumar, D.C. Neckers, Chem. Rev. 89 (1989) 1915–1925.
[23] E. Merino, Chem. Soc. Rev. 40 (2011) 3835–3853.
[24] N.E. Brese, M. O'Keeffe, Acta Crystallogr. Sect. B 47 (1991) 192–197.
[25] W.J. Randall, T.J.R. Weakley, R.G. Finke, Inorg. Chem. 32 (1993) 1068–1071.
[26] H. Li, P. He, R. Wan, et al., Dalton Trans. 49 (2020) 2895–2904.
[27] M. Lv, Y. Liu, K. Li, G. Yang, Tetrahedron Lett. 65 (2021) 152757.
[28] G. Yang, K. Li, X. Lin, et al., Chin. J. Chem. 39 (2021) 3017–3022.
[29] X. Liu, L. Cui, J. Jiang, F. Ji, J. Zhao, Chin. Chem. Lett. 33 (2022) 2630–2634.
[30] M. Cheng, Y. Liu, W. Du, et al., Chin. Chem. Lett. (2021), doi:10.1016/j.cclet.2021.11.059.
[31] M. Han, Y. Niu, R. Wan, et al., Chem. Eur. J. 24 (2018) 11059–11066.
[32] G. Yang, Y. Liu, X. Lin, et al., Chin. Chem. Lett. 33 (2022) 354–357.
[33] S. Han, Y. Cheng, S. Liu, et al., Angew. Chem. Int. Ed. 60 (2021) 6382–6385.
[34] Y. Gu, Q. Li, D. Zang, et al., Angew. Chem. Int. Ed. 60 (2021) 13310–13316.
[35] X. Zhou, H. Zhao, S. Liu, et al., Chin. Chem. Lett. 32 (2021) 761–764.